



# 1      **Hydroclimate reconstruction during the last 1000 years inferred by mineralogical and** 2      **geochemical composition of a sediment core from Lake-Azuei (Haiti)**

3      David Noncent<sup>1,2</sup>, Abdelfettah Sifeddine<sup>1,2,3</sup>, Evens Emmanuel<sup>1,2</sup>, Marie-Helene Cormier<sup>4</sup>,  
 4      Francisco J. Briceño-Zuluaga<sup>5</sup>, Mercedes Mendez-Milan<sup>2,3</sup>, Bruno Turcq<sup>2,3</sup>, Sandrine  
 5      Caquineau<sup>2,3</sup>, Jorge Valdés<sup>6</sup>, Juan Pablo Bernal<sup>8</sup>, John W. King<sup>4</sup>, Irina Djouaev<sup>3</sup>, Fethiye Cetin<sup>3</sup>,  
 6      Heather Sloan<sup>7</sup>

7      <sup>1</sup>ERC2, Université de Quisqueya, 218 Ave Jean-Paul II, 6110 Port-au-Prince, Haïti

8      <sup>2</sup>International Joint Research Laboratory CARIBACT. IRD-France and UEH-Haïti

9      <sup>3</sup>LOCEAN, IPSL, IRD-Sorbonne Université-CNRS-MNHN, Centre IRD France Nord, 32 Av.  
 10      Henri Varagnat, 93143 Bondy, France

11      <sup>4</sup>University Rhode Island, GSO Narragansett, RI, USA

12      <sup>5</sup>Faculty of Basic and Applied Sciences, New Granada Military University (UMNG), Bogotá  
 13      (Colombia)

14      <sup>6</sup>Laboratorio de Sedimentología y Paleoambientes, Instituto de Ciencias Naturales A. v.  
 15      Humboldt, Facultad de Ciencias del Mar y de Recursos Biológicos, Universidad de Antofagasta,  
 16      Antofagasta, Chile

17      <sup>7</sup>Lehman College, City University of New York, NY, USA

18      <sup>8</sup>Universidad Nacional Autónoma de México, Centro de Geociencias, Campus Juriquilla, 76001  
 19      Querétaro, QRO, México

20      **Correspondence:** David Noncent ([ndavid02@yahoo.fr](mailto:ndavid02@yahoo.fr))

## 21      **Abstract**

22      This study aims to reconstruct the hydro-climatic variations over the last 1000 yrs in Haiti using  
 23      mineralogical and geochemical composition of well dated lacustrine sediment core retrieved  
 24      from Lake Azuei. The results show changes in sedimentological processes linked to  
 25      environmental and climatic variations. The general pattern suggests a wetter Medieval Climate  
 26      Anomaly (MCA), drier Little Ice Age (LIA), high climate variability during the MCA-LIA  
 27      transition and more anthropogenic impacts that dominate natural climate during the Current  
 28      Warm Period (CWP). The MCA period (~1000-1100 CE) thus appears marked by increase  
 29      sedimentation rate supported by higher terrigenous input linked to erosive events and  
 30      consequently increases in precipitation. During the LIA, particularly from ~1450 CE to 1600 CE,  
 31      there is a great variation towards a decrease of terrigenous input, which is related to a decrease  
 32      on sedimentation rate and increase Mg-calcite precipitation, suggesting less precipitation and  
 33      high evaporation respectively during dry climate conditions. The MCA-LIA transition (~1200-  
 34      1400 CE) is characterized by variations between terrigenous input, Mg-calcite neoformation and  
 35      organic matter deposition, which indicate succession of dry and humid conditions. The CWP  
 36      (1800-2000 CE) shows a progressive increase on sedimentation rate and decrease of grey level,  
 37      which indicate more organic matter sedimentation as consequence of anthropogenic activities in



the surrounding basin of the lake. High-resolution grey level analysis, which reflects principally variations in terrigenous input, carbonate mineral neof ormation and organic matter deposition, shows that the AMO, NAO, PDO and ENSO are the principal modes affecting the hydro-climatic changes in Haiti during the last millennium. In addition, temporal correlation of other Caribbean paleoclimate records with our geochemical and mineralogical data, suggests that trends observed in Lake Azuei were controlled by regional climate, likely associated with shifts in the position of the ITCZ.

## 1. Introduction

The climate of the Caribbean region is subject to the influences of synoptic features of both tropical Atlantic and Pacific basins. Reconstructions of Caribbean climate during the last millennia offer a basis for understanding these influences, and better predicting future global climate. Some studies (Mann et al., 2009; Tierney et al., 2015) have shown that climate modes, particularly the Atlantic Multidecadal Oscillation (AMO) and North Atlantic Oscillation (NAO), the Pacific Decadal Oscillation (PDO) and El Niño-Southern Oscillation (ENSO), have influenced the hydro-climate changes during the last millennium. At the multidecadal timescale various studies (Mann et al. 2009, Knudsen et al. 2011, Apaestegui, et al., 2014) have shown that the tropical climate variability is driven by the interplay between AMO and PDO. In addition to these climate modes, the NAO affects rainfall patterns in the Caribbean through its influence on the strength and position of the North Atlantic Subtropical High (NAH) (Wang, 2007; Cook and Vizy, 2010) and consequently the Caribbean Low Level Jet (CLLJ) (Burn and Palmer, 2014). Mean annual precipitation in the northeastern Caribbean has also been shown to be synchronous with variations in the NAO, at least since 1914 (Malmgren et al., 1998). Furthermore, the amount of rainfall and their variability are also strongly modulated by changes in the Pacific climate mode including ENSO phenomenon (Chen et al. 1997; Giannini, Kushnir and Cane 2000; Taylor, Enfield and Chen 2002; Ashby, Taylor and Chen 2005; Gamble, Parnell and Curtis, 2008). Superimposed on those climate modes, which dominate the interannual variations observed over the last decades, Black et al., (2004) has shown that solar variability plays a role in influencing the hydrologic balance of the circum-Caribbean region.

In inter-tropical regions, variations in the hydrological cycle have more consequences than variations in temperature on physical ecosystems and systems such as lakes (Goosse and Klein, 2021) which are particularly sensitive to changes in hydro-climatic conditions. These impacts therefore leave important signals in the paleoclimatic records that allow us to reconstruct indices characterizing wet or dry conditions. The lacustrine sediments preserve several markers (organic, inorganic) which provide valuable information about the history of the surrounding basin's lake, its current state and its environment and consequently climate changes. The inorganic sedimentation process is therefore influenced by hydrological factors as erosion which can be linked to changes in precipitation and or human activities (agriculture, industrial wastewater, and mining activity) and mineral neof ormation under different physico-chemical conditions. Mineralogical elements composition and concentrations in sediments can vary depending on



77 natural abundance, intensity of precipitation and physico-chemical lacustrine water conditions,  
 78 morphology of lake surrounding basin and land use practices.  
 79 Curtis and Hodell (1993) and Higuera-Gundy et al. (1999), using pollen and isotopic  
 80 compositions of a sediment core from Lake Miragoâne in southwest Haiti, documented climatic  
 81 and environmental changes in Haiti during the last 10,500 years, and in particular, changes in the  
 82 precipitation regime. The results of geochemical evaluation of sediment and gastropod shells of  
 83 Lake Azuei indicated also there were changes in the precipitation regime during the last century  
 84 (Eisen-Cuadra, 2013). However, climate modes haven't been proposed to elucidate these  
 85 changes. In addition, to date, no detailed study has been done on climate variability during the  
 86 past millennium in Haiti. Therefore, more temporal and spatial data are needed to constrain Haiti  
 87 climate change.  
 88 The objective of this study is to reconstruct the climatic variability in Haiti during the last  
 89 millennium using mineralogical and geochemical composition. We also seek to understand  
 90 climate mechanisms and modes that could explain this variability.

## 91 Study site

92 The sediment core LA17BCO2 was collected in January 2017 from Lake Azuei, also known as  
 93 “*Étang Saumâtre*” (Fig. 1). This Lake, which is the largest lake in Haiti and the second largest  
 94 lake in Hispaniola, is located in the Cul-de-Sac watershed, around 29 kilometers east of Port-au-  
 95 Prince. Its area has experienced a remarkable increase since the end of the 20<sup>th</sup> century. It  
 96 fluctuated between 113 and 118 km<sup>2</sup> from 1985 to 2002. Then, starting in 2003, it increased by  
 97 about 15% compared to its 1985 level. It reached an area of 132 km<sup>2</sup> in 2011 (Romero and  
 98 Poteau, 2011) and 137 km<sup>2</sup> in 2014 (Moknatian et al., 2017), that corresponds to an increase of  
 99 4m of the water lake level. The lake level has been relatively stable since 2014. These dramatic  
 100 changes in lake level are echoed with other lakes in Hispaniola, including  
 101 Lake Enriquillo and Lake Miragoâne, and have been attributed to changing seasonal  
 102 rainfall patterns (Moknatian and Piasecki, 2019).

103 Lake Azuei is 22 km long, from northwest to southeast; its maximum width is 12 km and it  
 104 measures 30 m at its deepest (James et al., 2019). It is located in one of the driest regions of the  
 105 country (Moron et al., 2015) due to the Cordillera Central rain shadow effect. The lake is  
 106 endorheic, which means that its level is extremely sensitive to variations in precipitation. It is  
 107 located in an alluvial plain (Cul-de-Sac) bordered by mainly carbonate mountain. It lies along the  
 108 boundary between the North American and Caribbean plates, which are moving at a rate of 19  
 109 mm/yr relative to each other (Benford et al., 2012).

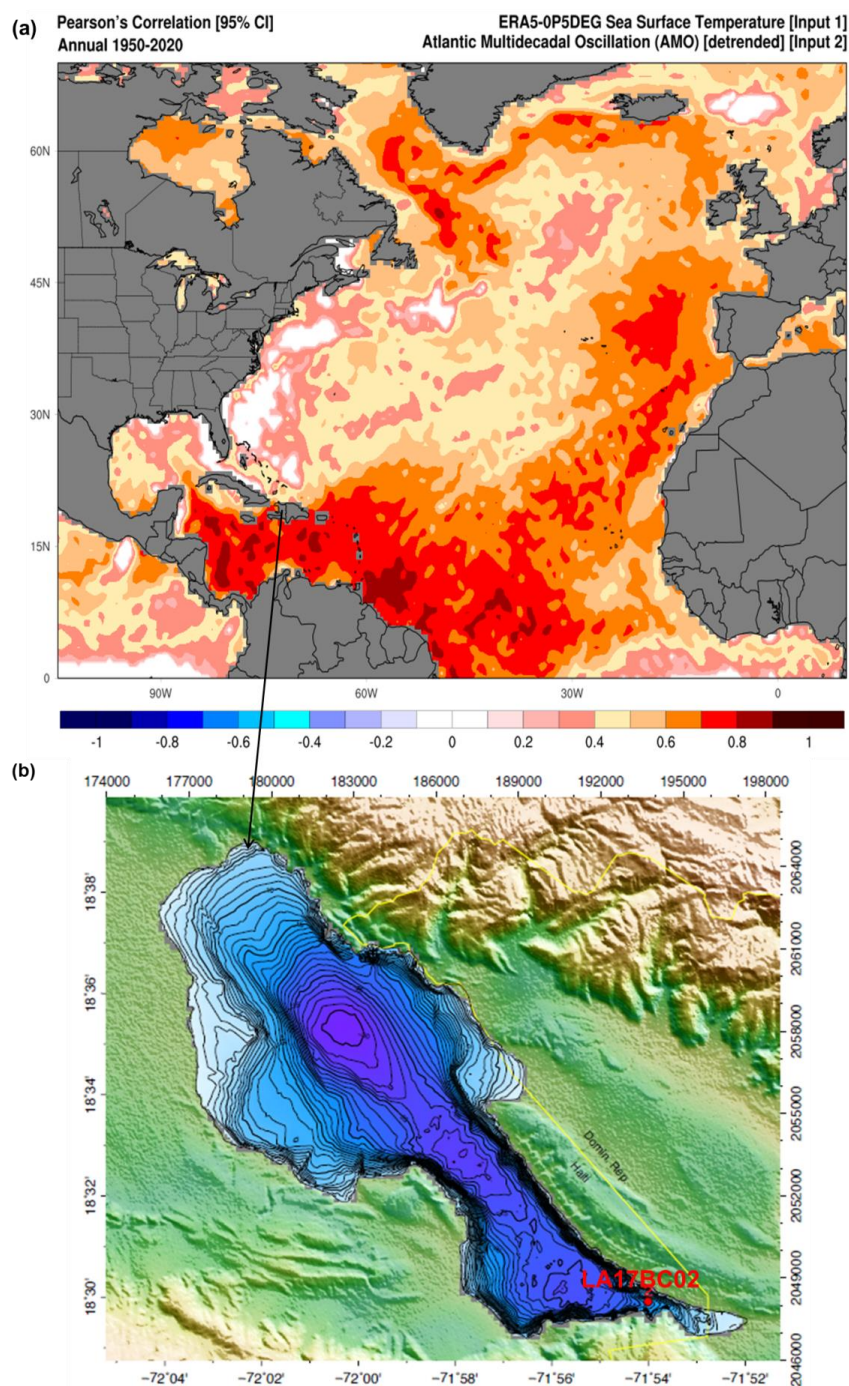


Fig. 1: (a) Spatial correlation between instrumental AMO and Sea Surface Temperature (SST) from ERA5-OP5DEG from 1950 to 2020. (b) Bathymetric chart compiled from depth soundings





collected between 2013 and 2017 (Cormier et al., 2018). Contour interval is 1 m. Yellow line indicates the Haitian-Dominican border

## 2. Materials and method

### 2.1. Lake sediment Coring

Coring system used was provided by the NSF National Facility “LacCore” at the University of Minnesota-Minneapolis. The core LA17BCO2, 84 cm length, was collected at 19.8 m of water depth using the Bolivia corer which is a piston rod corer. Its GPS coordinates are 18 ° 30.0931' N, 71 ° 54.0302' W. The core sub-sampling campaign was carried out at the Graduate School of Oceanography at Rhode Island University, United States. The samples were taken every two centimeters, except in some level where samples had already been taken for radio-isotope dating. In total, 32 samples were taken from the core for the geochemical and mineralogical analysis.

### 2.2. Dating

Gastropod shells, wood and bulk organic matter sediments were dated by  $^{14}\text{C}$  using mass accelerator spectrometer. Dating of gastropod shells and wood was performed in the U.S.A at the Beta Analytical Laboratory, Miami, Florida, and at the NOSAMS facility in Woods Hole, Massachusetts. Dating of bulk organic matter sediment was carried out at the LMC14 laboratory, Saclay, Paris, France. To date the upper part of the core more precisely, activities of  $^{210}\text{Pb}$  (unsupported Pb) were carried out at the University of Rhode Island every centimeter over the upper 10 centimeters. Because atmospheric radiocarbon production has varied over geologic time, radiocarbon ages have been calibrated to provide dates in years CE. Thus, Calibrated ages (2 sigma) in “approximate calendar” years were obtained from Stuiver et al. (1998) by means of the calibration program CALIB 8.2 software (Stuiver and Reimer, 2022).

### 2.3. Lithology and grey level analysis

The physical characteristics such as color, the existence of bands and laminae structures have been realized by observation both at the macroscopic and microscopic scales. Grey levels were measured using Image software on a high resolution photo of the core taken at the University of Rhode Island. The image software, ImageJ, is a Java-based image processing program developed at the National Institutes of Health and the Laboratory for Optical and Computational Instrumentation (LOCI, University of Wisconsin). The grey level was set from 0 to 255. Larger numbers imply brighter colors.

### 2.4. Inorganic compositional analysis.

Major and trace (Ca, Al, Fe, K, Ti, Zr) element concentrations were analyzed by ICP-MS (Agilent 7500 cx) at IRD, LOCEAN, Bondy, after acid digestion following the methodology used by Valdés et al. (2014) : 1) samples weighing 20 to 25 mg into savilex vessel were treated with a combination of nitric acid ( $\text{HNO}_3$ ) and hydrofluoric acid (HF), followed by heating at 150



148 °C for 48h; 2) HF and perchloric acid (HClO<sub>4</sub>) solution was added and digested at 150°C for 24  
 149 h ; 3) HNO<sub>3</sub> attack was done twice at 150 °C to evaporate all acid from the samples; 4) the  
 150 resulting material was brought to 35 mL with HNO<sub>3</sub>. The analytical procedure was controlled by  
 151 the routine replicate analysis, target material, and MESS-3 certified reference material. The  
 152 analytical validation data showed accuracy with a relative error that did not exceed 5%.

### 153 **2.5. Mineralogical analysis.**

154 The mineralogical composition was determined by X-ray diffraction (XRD) at IRD, LOCEAN,  
 155 Bondy, using a PANalytical X'Pert powder diffractometer with Ni-filtered CuK $\alpha$  at 40kV and  
 156 40mA, equipped with a PIXcel detector. Samples, previously ground with an agate mortar were  
 157 prepared as randomly oriented powder mounts and scanned from 2 to 70° (2 $\theta$ ) with a step size of  
 158 0.0131 °2 $\theta$ . Mineral identification was performed using the Highscore 3.0 software  
 159 (PANalytical®) and two databases: ICSD (Inorganic Crystal Structure Database) and COD  
 160 (Crystallography Open Database).  
 161 Estimation of the contribution of the main detected minerals was achieved by using the integrated  
 162 peak area of the most intense diffraction peak of calcite (d<sub>104</sub>, 3.03 Å), Mg-calcite (d<sub>104</sub>, at 2.99  
 163 Å), aragonite (d<sub>111</sub>, 3.40 Å), quartz (d<sub>101</sub>, 3.34 Å) and clays (represented by a common diffraction  
 164 peak at 4.50 Å). The relative contribution of each mineral, expressed as a percentage of the sum  
 165 of all the measured peak areas, does not represent a mass percentage but allow following the  
 166 variability of the mineralogical composition along the core.

### 167 **2.6. Organic carbon analysis.**

168 Organic carbon content (C<sub>org</sub>) was measured with an elemental analyzer Flash 2000HT from  
 169 Thermo Fischer Scientific coupled to a thermal conductivity detector (TCD) at LOCEAN,  
 170 Bondy, France. Each sample was weighted in a precision balance and placed in tin capsules.  
 171 Prior to the analyses, carbonates were removed with hydrochloric acid 10%.

## 172 **3. Results**

### 173 **3.1. Chronology and sedimentation rate**

174 Ten <sup>14</sup>C measurements by AMS (Table 1) were made on 3 samples consisting of gastropod  
 175 shells, 1 wood sample, and 6 bulk sedimentary organic carbon samples. In addition, <sup>210</sup>Pb dating  
 176 (Table 2) was made every cm in the upper 7 cm of the core allowing estimating an age of ~48  
 177 years BP (1970 CE) between 6 and 7 cm (Table 1).

178 **Table 1. Sediment Depth-Age Relations using dating <sup>14</sup>C for LA17BCO2**



Laboratory	Depth (cm)	Sample (material)	Age 14C (BP)	Calibration	Reservoir corrected 14C age BP	Calibrated Age 2σ (CE)
NOSAMS-USA	6-7	AMS <sup>14</sup> C gastropod	2680 +/- 25	IntCal20	48 +/- 25	1970
LMC14-France	10-11	Sediment	2465 +/- 25	IntCal20	115 +/- 25	1870
LMC14-France	16-17	Sediment	2595 +/- 35	IntCal20	245 +/- 30	1715
LMC14-France	28-29	Sediment	2730 +/- 30	IntCal20	490 +/- 30	1430
Beta-Analytic-USA	42-43	AMS 14C wood	990 +/- 30	IntCal20	990 +/- 30	1130
Beta-Analytic-USA	42-43	AMS 14C gastropod	3230 +/- 30	IntCal20	990 +/- 30	1120
LMC14-France	56-57	Sediment	2860 +/- 30	IntCal20	620 +/- 30	1310
Beta-Analytic-USA	63-64	AMS 14C gastropod	2970 +/- 30	IntCal20	730 +/- 30	1280
LMC14-France	68-69	Sediment	3275 +/- 30	IntCal20	1035 +/- 30	750
LMC14-France	81-82	Sediment	3110 +/- 30	IntCal20	870 +/- 30	1200

179 Lake Azuei is a hard-water lake varying in hardness between 525-2260 mg/l of CaCO<sub>3</sub> (Matthes,  
 180 1988). Consequently the radiocarbon dates of shells and bulk sedimentary organic carbon are  
 181 subjected to errors resulting from the dilution of <sup>14</sup>C by “old” carbon (i.e. <sup>14</sup>C-free) which is  
 182 derived from the dissolution of calcareous bedrock; this is called “hard - water - lake error  
 183 (HWLE)”. Taking into account the dates of <sup>210</sup>Pb, activities of <sup>137</sup>Cs and the gastropods for the 6-  
 184 7 cm interval and those of wood and gastropods for the 42-43 cm interval, three corrections of  
 185 hard water effect can be estimated. In the upper part (6-7 cm), a HWLE of 2630 yrs BP was  
 186 removed from the <sup>14</sup>C date. From 10 to 17 cm, a HWLE of ~2350 yrs BP was removed from the  
 187 <sup>14</sup>C dates. Below 28 cm, they are subtracted from 2240 yrs BP based on the dating of the wood  
 188 sample.

189 **Table 2. Sediment Depth-Age Relations for using dating <sup>210</sup>Pb for the upper of LA17BCO2**

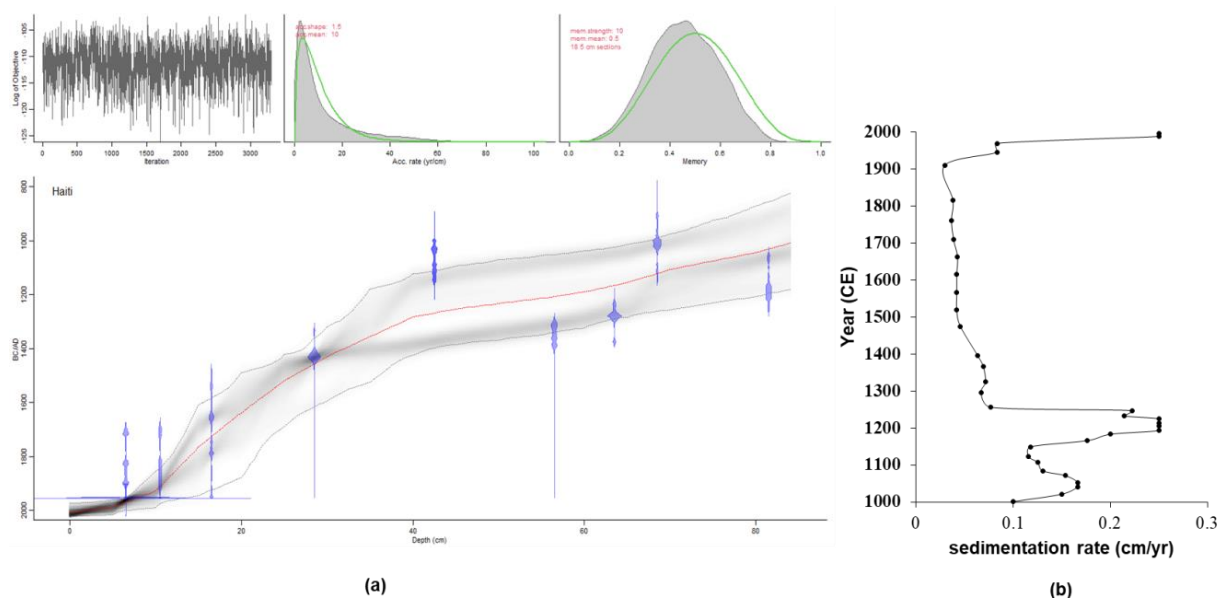
Depth (cm)	<sup>210</sup> Pb <sub>xs</sub> (dpm/g)	ln ( <sup>210</sup> Pb <sub>xs</sub> )
0-1	2.717	1
1-2	1.791	0.583
2-3	1.482	0.393
3-4	0.987	-0.013
4-5	0.884	-0.124
5-6	0.698	-0.359
6-7	0.694	-0.365

190 <sup>210</sup>Pb and radiocarbon dates were combined to form a Bayesian age-depth model using the  
 191 rBacon package within R (Blaauw and Christen 2010). Mean ages were extracted from the model



192 and used for the representation and interpretation of the proxy data. Observing the graphical  
 193 representation of the age-depth used to establish the chronology (Fig. 2a).

194



195

196 Fig. 2: (a) Bayesian age-depth model for core LA17BCO2 generated using rBacon for R,  
 197 displaying  $^{14}\text{C}$  dates corrected for HWLE. The jagged blue error bars display the  $^{14}\text{C}$  age  
 198 probability distribution for each sample; the dotted red line follows the mean ages. In detail at  
 199 the top from left to right; number of iterations, sedimentation rate and memory, this is interpreted  
 200 as the dependence of the accumulation rate between neighboring depths. (b) Sedimentation rate  
 201 (cm/yr) calculated from age-depth model. Average sedimentation rate in sediment core  
 202 determined with the age-depth model (Fig. 2b), was  $0.128 \pm 0.079$  cm/yr. The higher values are  
 203 observed between: 84 to 76 cm (1000 to 1150 CE), 68 to 41 cm (1100-1250 CE) and 10 to 0 cm  
 204 (1900-2000 CE). From 38 to 10 cm (1300 to 1900 CE) we observed a trend to decrease of  
 205 sedimentation rate.

### 206 3.2.Lithology and grey level

207 Based on the visual characteristics of the sediments, different stratigraphic levels could be  
 208 identified for LA17BCO2 (Fig. 3, core image). The different levels were characterized either by  
 209 the clay facies or by frequent alternation of organic matter within clayey to homogeneous silty  
 210 levels or by less frequent alternation of organic matter and a more silty level. The upper levels  
 211 have a much darker color, therefore much richer in organic matter. The macrofauna is mainly  
 212 composed of gastropods. In the middle of the core there is a particularly high concentration of  
 213 gastropods. Overall, microscopic observation of some samples indicates that the sediment facies

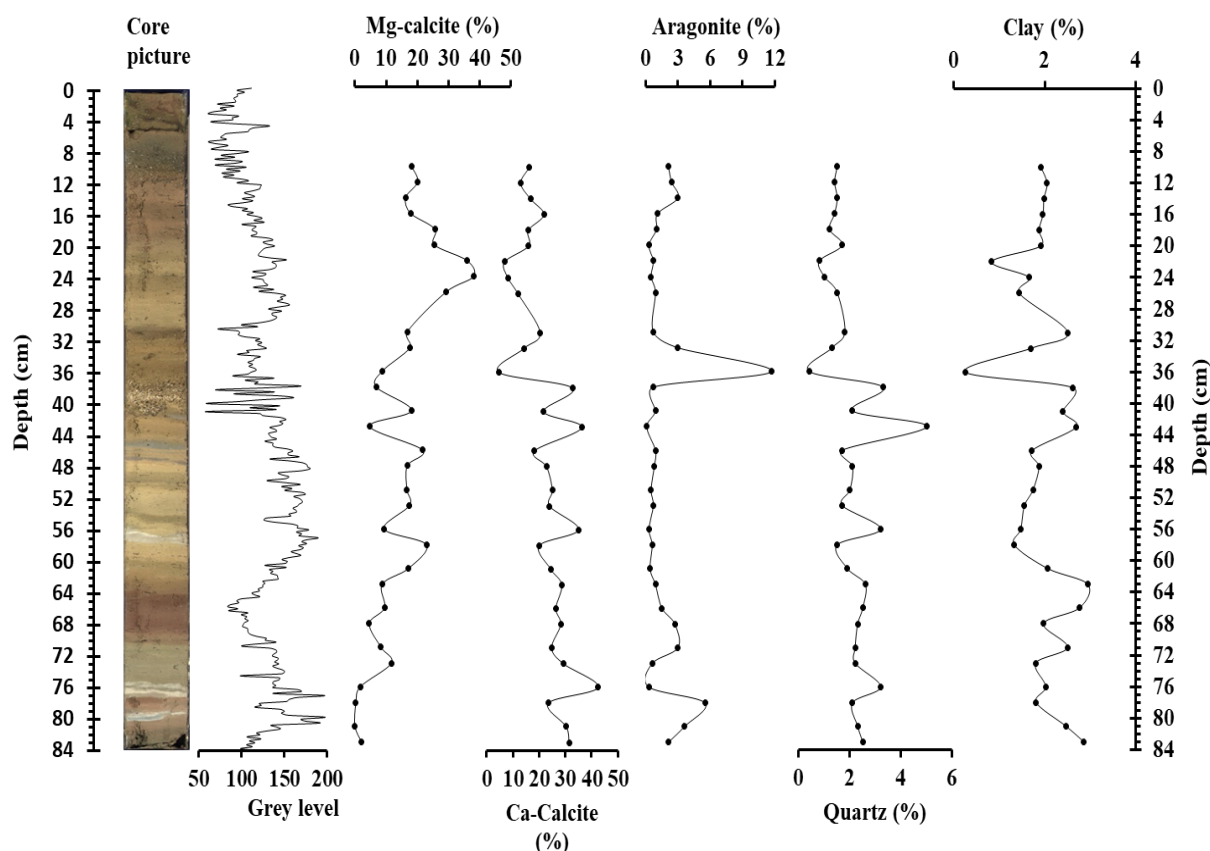




214 contain fine grains of authigenic limestone, suggesting that the coring site is well protected,  
 215 allowing only the transport and deposition of fine particles (clays, silts). Sediment deposition  
 216 occurred in a low energy environment. Amorphous and fluorescent organic matter is also  
 217 present. Some plant debris were observed.

218 The observed grey level values varied between 32 (darker) and 240 (brighter). The grey level  
 219 data exhibit high variations in different level of the core (Fig. 3). Brighter colors were found in  
 220 the lower part of the core than in the upper part. Highest values are recorded for two intervals,  
 221 between 80 to 72 cm, and 60 to 48 cm. From 42 to 36 cm grey level show high fluctuations  
 222 between low and high grey level values. Finally, a tendency towards a decrease of grey level  
 223 values was observed from 28 cm and reaches the minimum between 12 cm and the top of the  
 224 cores.

### 225 3.3. Variation of the mineralogical composition

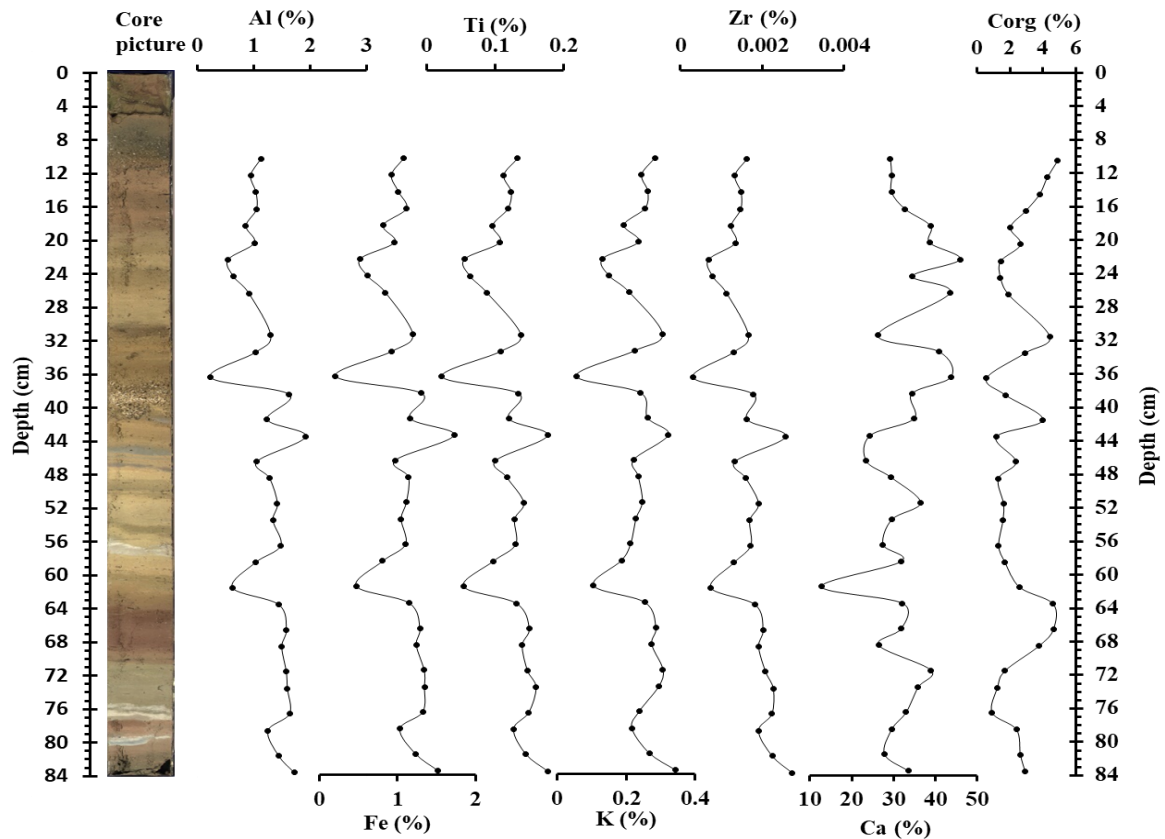


226 Fig. 3 Core picture; lithological profile, grey level variation, and distribution of the mineral  
 227 content expressed as a peak area percentage of the core LA17BCO2 are plotted against depth.  
 228



229 The mineralogical composition of the different samples is homogeneous. The most prominent  
230 mineral phase throughout the core consists of carbonates: Calcite ( $\text{CaCO}_3$ , called here Ca-  
231 calcite), Mg-calcite ( $\text{Mg}_x\text{Ca}_{1-x}\text{CO}_3$ ) and aragonite ( $\text{CaCO}_3$ ). The peak area percentages of Ca-  
232 calcite, Mg-calcite, aragonite, quartz and clays are shown in Fig. 3. Ca-calcite, quartz and clays  
233 are three from lithogenic inputs, they have the same behaviour and and strongly positively  
234 correlated (Fig. 3, Table 3). By contrast, Mg-calcite has an exact opposite behaviour as quartz,  
235 clays and Ca-calcite. For aragonite, there is almost no variation in its proportions in the different  
236 levels except a slight increase in the 36 cm.

237 *3.4. Variation of the geochemical composition*



238  
239 Fig. 4 The temporal variations of the geochemical composition (core LA17BCO2) of Lake  
240 Azuei.

241 The most abundant major element in the lake sediments is Ca, in agreement with the high calcite  
242 (Ca-calcite and Mg-calcite) content (Fig. 3). Following in order of abundance are Al, Fe, K, Ti  
243 and Zr. Indeed, the average percentages of the elements analyzed: Ca, Al, Fe, K, Ti, Zr, are,



244 respectively,  $32.48 \pm 5.06$  %,  $1.21 \pm 0.31$ %,  $1.05 \pm 0.22$  %,  $0.23 \pm 0.04$  %,  $0.12 \pm 0.03$  %, and  
 245  $0.0016 \pm 0.00004$  %; with a maximum value at 43 cm and a minimum values at 36 cm.  
 246 Variations in concentrations Al, Fe, K, Ti and Zr are correlated as confirmed by the coefficient  
 247 of Pearson (Fig. 4, Table 3). At the bottom of the core between 83 and 76 cm, there is a tendency  
 248 towards a decrease in their concentrations with an inflexion at 78 cm. From 78 to 76 cm their  
 249 concentrations increase. From 63 to 61 cm there is a decrease in concentrations which will  
 250 subsequently increase up from 61 to 56 cm. From 56 to 46 cm there is little variation in  
 251 concentrations with a slight tendency to increase. From 48 to 43 cm we observed an increase of  
 252 their concentrations. From 43 to 31 cm there is a great variation of them with a peak at 31 cm.  
 253 Thus, elements concentrations decrease from 43 to 36 cm and increase from 36 to 31 cm. From  
 254 31 to 22 cm, elements concentrations decrease. From 22 to 10 cm, there is a weak variation of  
 255 the elements unlike the variations in the downcore. The greatest amplitude of the variation in the  
 256 concentrations of elements is observed between 46 and 22 cm. On the other hand, Ca  
 257 concentrations vary in opposition to Al, Fe, K, Ti and Zr concentrations in the upper half of the  
 258 core: From 48 to 10 cm, where Ca concentrations increase, there is decrease in Al, Fe, K, Ti and  
 259 Zr concentrations.

260 The organic carbon content,  $C_{org}$ , varies in a narrow range from 0.6 % to 4.9 % (average of  $2.5 \pm$   
 261  $1.22$  %). It is highly variable and trend to increase in the topmost sediments.  $C_{org}$  varies in an  
 262 opposite trend to Ca (Fig. 4).

## 263 **4. Discussion and interpretation**

264 The results are discussed and interpreted globally according to three major periods that have  
 265 marked the climate during the last millennium: Medieval Climate Anomaly (MCA, 1000-1100  
 266 CE), the Little Ice Age (LIA, 1450-1800 CE) and the Current Warm Period (CWP, from 1850  
 267 CE to present) (Bird et al., 2011).

### 268 **4.1. Terrigenous input (Detrital input)**

269 A Pearson correlation analysis (Table 3) confirms a positive correlation between the terrigenous  
 270 fractions (Al, Fe, Ti, K, and Zr), and their negative correlation with Ca. Indeed, Al, Fe, Ti, K and  
 271 Zr correlate well with each other indicating that all those elements are from the same source area.  
 272 They also show similar variations (Fig. 4), suggesting that regional scale processes affect the  
 273 input of these elements into the lake. K, Ti and Zr are significantly correlated to Al and Fe  
 274 confirming their common and crustal origin. In addition, Al, Fe, Ti, K, and Zr are strongly  
 275 correlated with the Ca-calcite content (Fig. 5, Table 3) and the detrital minerals (clays and  
 276 quartz) (Table 3), suggesting their common origin, and negatively correlated with the Mg-calcite



277 content. Lower Mg-calcite contents correspond to higher proportion of the other minerals (Fig.  
 278 3).

279 **Table3. Pearson's correlation coefficient matrix between metals and mineral compositions**

Variables	Al	Ti	Fe	Zr	K	Clays	Quartz	Ca-Calcite	Mg-Calcite	Ca
<b>Al</b>	1									
<b>Ti</b>	0.957	1								
<b>Fe</b>	0.965	0.973	1							
<b>Zr</b>	0.959	0.975	0.955	1						
<b>K</b>	0.844	0.938	0.930	0.875	1					
<b>Clays</b>	0.716	0.728	0.760	0.710	0.762	1				
<b>Quartz</b>	0.843	0.722	0.792	0.759	0.559	0.625	1			
<b>Ca-Calcite</b>	0.871	0.771	0.780	0.824	0.559	0.606	0.876	1		
<b>Mg-Calcite</b>	-0.670	-0.623	-0.596	-0.702	-0.443	-0.451	-0.631	-0.748	1	
<b>Ca</b>	-0.258	-0.241	-0.231	-0.237	-0.179	-0.396	-0.403	-0.445	0.315	1

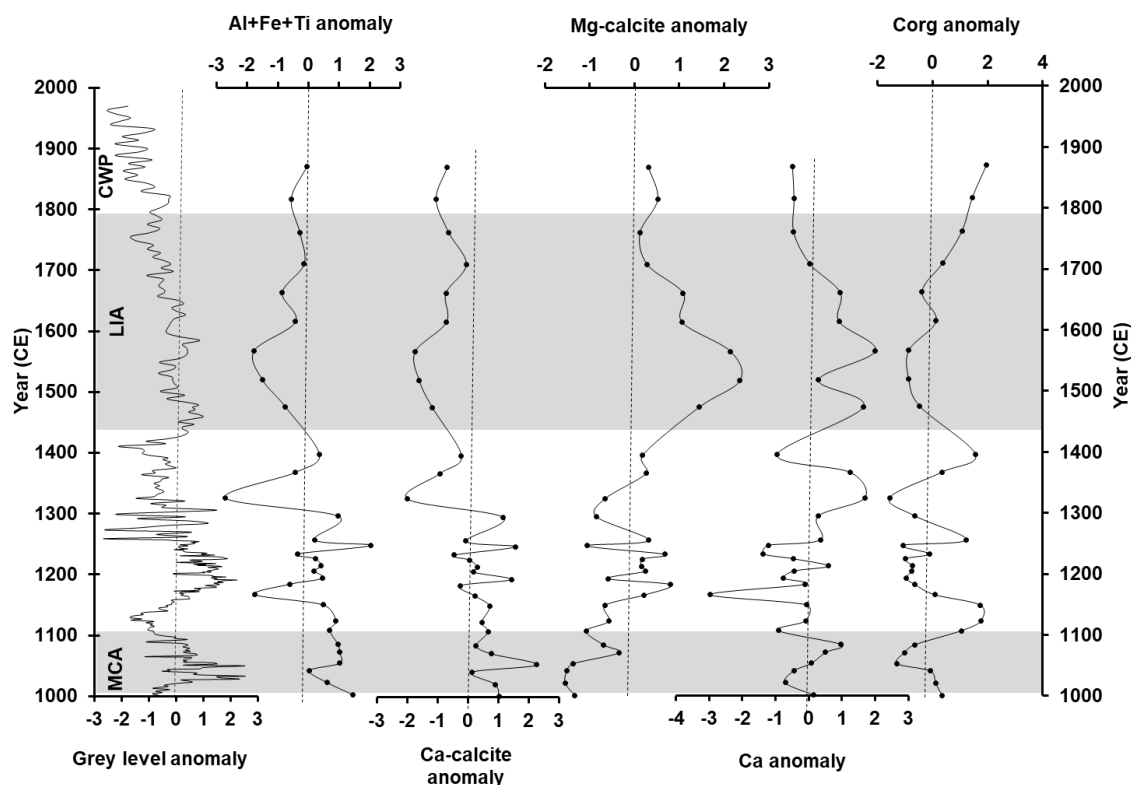
280 One of the first parameters that can strongly influence the concentrations of elements  
 281 independently of the redox conditions or the productivity of the environment at the time of  
 282 deposition is terrigenous input. Indeed, parts of the elements of most sediment are of detrital  
 283 origin (Tribovillard et al., 2006). The impact of detritus on the concentrations of the studied  
 284 elements would be verified if their concentrations were correlated to that of aluminum (Calvert  
 285 and Pedersen, 1993; Hild and Brumsack, 1998; Böning et al., 2004; Tribovillard et al., 2006), as  
 286 is indeed the case for our measurements (Table 3). These elements are therefore mainly of  
 287 detrital origin and can be used to interpret the depositional conditions. Al, Fe, Ti, K and Zr  
 288 variations in the Lake Azuei are not diagenetically controlled, and can be interpreted to reflect  
 289 changes in terrigenous inputs and the pedogenic processes occurring in the surrounding basin.  
 290 The variations of Al, Fe, Ti, K and Zr content in the sediment will thus be interpreted as a proxy  
 291 of soil erosion, with low concentrations indicating less transport and, conversely, high  
 292 concentrations indicating more transport to the lake. Indeed, the MCA period (1000-1100 CE) is  
 293 characterized by positive anomalies of terrigenous input (Fig. 5), related to detrital input in the  
 294 lake. The MCA-LIA transition (1200-1400 CE) is characterized by variations between positive  
 295 and negative anomalies of terrigenous input. However, the LIA (1400-1800 CE) period is  
 296 characterized by negative anomalies of terrigenous input (Fig. 5), related to less detrital input in  
 297 the lake. Additionally, some periods characterized by positive (negative) anomalies for the sum  
 298 of Al, Fe and Ti, display negative (positive) anomalies of Ca (Fig. 5). The negative anomalies of  
 299 Ca may be the result of increased dilution by terrigenous particles derived from erosion  
 300 (Baumann et al., 1993). On the other hand, the positive anomalies of Ca are linked to  
 301 precipitations of calcium carbonates when there is a decrease in terrigenous elements (negative  
 302 anomalies of sum Al, Fe, and Ti).



#### 303 **4.2. Calcite neoformation.**

304 Several studies have explained the formation and sedimentation processes of calcium carbonate  
 305 in lakes (Müller et al., 1972; Müller and Wagner 1978; Last, 1982; Effler and Johnson, 1987;  
 306 Last and De Deckker, 1990; Queralt et al., 1997; Elfil and Roques, 2001; Gal et al., 2002; Morse  
 307 et al., 2007; Dean et al., 2009; Solotchina and Solotchin, 2014; Tompa et al., 2014). Various  
 308 calcium carbonate minerals may occur in the aquatic environment either as primary carbonates  
 309 or as the results of diagenetic processes in the sediments. Lake water temperature and its  
 310 concentration in Mg:Ca ratio are the two main factors that determine the composition and  
 311 crystallographic variety of precipitated calcium carbonate: Ca-calcite, aragonite, Mg-calcite  
 312 (Müller et al., 1972; Kelts and Hsui, 1978; Morse et al., 2007; Dean et al., 2009). Temperature  
 313 not only affects biogenic factors but also the solubility of CO<sub>2</sub> in water (Schwoerbel, 1999).  
 314 Also, through temperature-dependent evaporation the total volume of water influencing the ion  
 315 concentration within the lake is modified. Calcite is the most stable crystalline variety of  
 316 calcium carbonate at ambient temperature and pressure, with aragonite being stable at high  
 317 pressure (Cölfen, 2003; Nan et al., 2007). Last (1982) showed that the incorporation of  
 318 significantly higher amounts of Mg in the calcite lattice to form Mg-calcite is associated with  
 319 increased water temperature. In addition, the little different atomic radius of the Ca<sup>2+</sup> and Mg<sup>2+</sup>  
 320 cations, the identical crystalline structure of their carbonate (rhombohedral), their charges and  
 321 their similar electronegativities are all factors favorable to the formation of Mg-calcite instead of  
 322 calcite (Ca-calcite) with an increase in water temperature (Müller et al., 1972; Last and De  
 323 Deckker, 1990; Queralt et al., 1997; Morse et al., 2007). The opposite variations of Ca-calcite  
 324 and Mg-calcite in the Lake Azuei sediments (Fig. 5) can be used to interpret changes in water  
 325 temperature, and thus used as a proxy of water lake evaporation. During the LIA period (1400-  
 326 1800 CE), we observed positive anomalies for the Mg-calcite and negative anomalies for the Ca-  
 327 calcite, indicating that the lake water was warmer than during the MCA period (1000-1100 CE),  
 328 which is characterized by negative and positive anomalies for Mg-calcite and Ca-calcite,  
 329 respectively. The MCA-LIA transition (1200-1400 CE) is characterized by variations between  
 330 negative and positive anomalies of Mg-calcite.



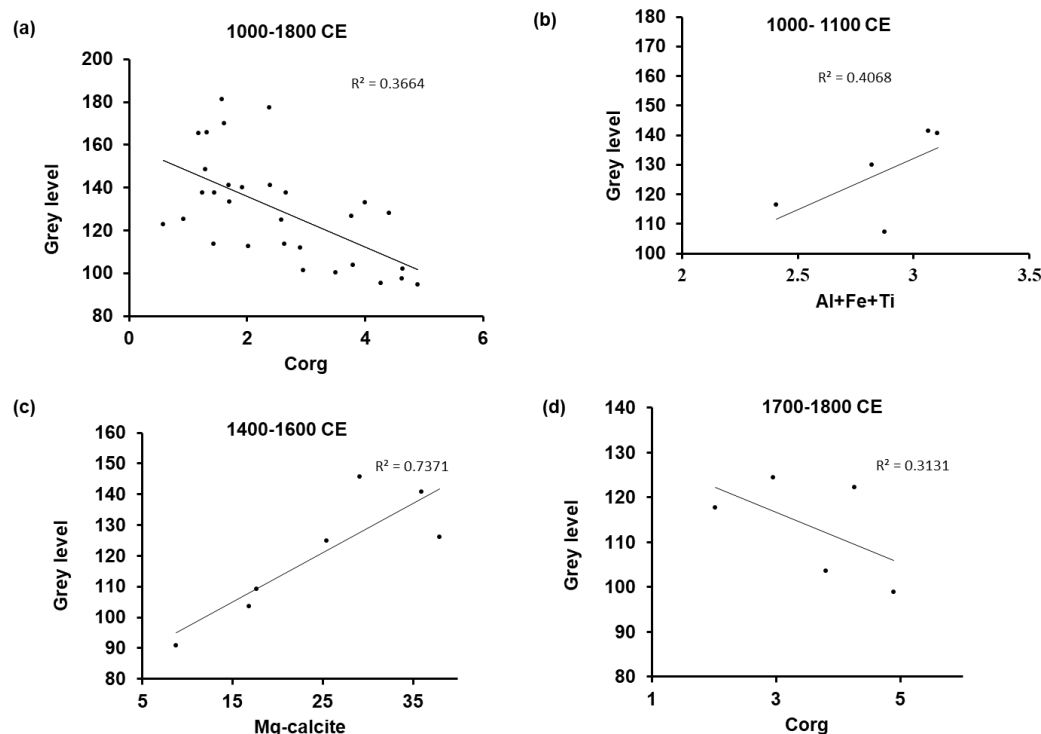


331

332 Fig.5 Temporal variations in grey level intensity, terrigenous input (% Al + % Fe + % Ti), Ca-  
 333 calcite, Mg-calcite, Ca and  $C_{org}$  in sediment core LA17BCO2 of Lake Azuei. The time scale  
 334 along the vertical axis is derived from the age-depth model displayed in Fig. 2a.

#### 335 4.3. Grey level correlation with proxies

336 The grey level reflects the combination of all materials (organic as well as inorganic) present in  
 337 the core sediment. Thus, its variation depends on the variations of these materials according to  
 338 their sedimentation conditions. Indeed, the grey level intensities exhibit a somewhat similar  
 339 variability to that of the terrigenous elements and calcite neoformation (Fig. 5). The lighter  
 340 (darker) colors coincide with more (less) terrigenous input and Ca-calcite precipitation. The  
 341 agreement between grey level and inorganic input (terrigenous and neoformation of Ca-calcite)  
 342 is supported by a negative correlation between grey level and  $C_{org}$  ( $r = -0.6$ , Fig. 6a), suggesting  
 343 that their variations may be controlled by the same environmental parameters.



344

345 Fig. 6 Correlation between grey level and: (a) organic carbon from 1000 to 1870 CE, (b)  
 346 terrigenous input from 1000 to 1100 CE, (c) Mg-calcite composition from 1400 to 1600 CE, (d)  
 347 organic carbon from 1700 to 1800 CE

348 The positive anomalies of grey level from 1000 to 1100 CE are more explained by terrigenous  
 349 input (Fig. 6c). From 1200 to 1400 CE, high fluctuations of grey levels values suggest there were  
 350 fluctuations between terrigenous input to the lake, precipitation of calcite and organic matter  
 351 deposition. The period from 1400 to 1600 CE, exhibits positive anomalies of grey level values  
 352 more controlled by Mg-calcite and aragonite precipitation (Fig. 6b), which indicate changes in  
 353 physico-chemical changes in water column conditions. Afterwards, the decrease of grey level is  
 354 more correlated with organic matter deposition (Fig. 6d). Indeed, from 1700 CE we observe an  
 355 increase in  $C_{org}$  content and the grey level shows darker colors. This input of  $C_{org}$  into the lake  
 356 could be due to deforestation resulting from the establishment of sugar cane plantations. Indeed,  
 357 in the 18<sup>th</sup> century, large sugar refineries developed in Haiti, which required groupings of land by  
 358 ten hectares (Cauna, 2013). The main sugar cane plantation sites were the great plains of the  
 359 country, including the Cul-de-Sac plain. Plantations were present almost everywhere around  
 360 Lake Azuei

#### 361 4.4. Hydroclimate interpretation and Comparison with other regional records



362 In order to gain insights into the dynamical link between the climate and the dominant modes of  
 363 variability, we applied wavelet analysis (Fig. 7j). This analysis reveals decadal and multi-decadal  
 364 spectral wavelets which could be associated with ENSO, PDO and AMO, respectively. In  
 365 addition a spectral analysis of average wavelet power of our record indicate an oscillation with  
 366 period periods in  $\sim 20$ ,  $\sim 64$ ,  $\sim 128$  years which could be related to PDO, AMO and some multi-  
 367 decadal variability respectively (Fig. 8).

368 Trend toward negative anomalies for both terrigenous inputs (Fig. 7a) and grey levels (Fig. 7b)  
 369 and positive anomalies for Mg-calcite/Ca-calcite ratio (Fig. 7c) in sediment of Lake Azuei from  
 370 1000 to 1800 CE suggests a progressive decrease in precipitation in Haiti over this period.  
 371 Indeed, proxy indicators suggest trends to dry conditions. Results from other studies in the circum-  
 372 Caribbean region contain also evidence for this trend. The oxygen isotope and Sr/Ca records from  
 373 Lake Miragoâne (Haiti) reveal a trend towards higher salinity conditions during the last millennium,  
 374 which is linked to an increase in the E/P ratio and therefore to dry conditions (Curtis et al.,  
 375 1993). The sediment titanium composition from the Cariaco Basin (Venezuela) (Haug et al.,  
 376 2001, Fig. 7d) show also a trend to more negative anomalies, related to a decrease in  
 377 precipitation patterns. The higher-resolution *G. ruber*  $\delta^{18}\text{O}$  record spanning the last 2000 years  
 378 from the Cariaco Basin show a trend toward more positive values that reflect a decrease SSTs  
 379 and an increase SSSs over the Caribbean and tropical North Atlantic (Black et al. 2004, Fig. 7e).  
 380 Indeed, the  $\delta^{18}\text{O}$  value of foraminiferal calcite is a function of temperature and salinity, whereby  
 381 an increase in  $\delta^{18}\text{O}$  is associated with a decrease of SST and an increase of SSS, and vice versa.  
 382 These studies thus indicate a decreasing precipitation over the circum-Caribbean that may be  
 383 associated with a southward migration of the ITCZ during this period. Indeed, Lechleitner et al.  
 384 (2017) have shown a trend to more southerly mean annual position of ITCZ from 1000 to 1800  
 385 CE. Thus, in Haiti the precipitations at secular scale are also controlled by the migration of the  
 386 ITCZ. The overall correlation between the terrigenous inputs in Lake Azuei, the *G. ruber*  $\delta^{18}\text{O}$   
 387 record (Black et al. 2004) and the sediment titanium composition from the Cariaco Basin (Haug  
 388 et al., 2001) show that the Caribbean region observed a common climate pattern over the past  
 389  $\sim$ millennium.

390 The MCA period appears marked by positive anomalies for terrigenous input linked to positive  
 391 anomalies for grey level (Fig. 7a, 7b), which have been confirmed by increase in sedimentation  
 392 rate (Fig. 2b). This tendency was likely related to the pattern of rainfall and runoff from the  
 393 surrounding watershed and suggests an environment characterized by wet conditions. The  
 394 negative Mg-calcite/Ca-calcite ratio anomaly recorded during this period (Fig. 7c), indicates a  
 395 low Mg-calcite concentration in sediment which related to a low evaporation of the lake water.  
 396 This is consistent with other proxy records from the northern tropical Americas, including the  
 397 Yucatan (Hodell et al., 2005), the Gulf of Mexico (Richey et al., 2007), lowland Venezuela  
 398 (Curtis et al., 1999), and the Cariaco Basin (Haug et al., 2001; Black et al., 2004), and the Las  
 399 Lagunas (Castilla, Felipe, Clara, Salvador) in Dominican Republic (Lane et al., 2009). The Las  
 400 Lagunas sediment records provide evidence of a relatively wet MCA in the eastern Caribbean  
 401 (Lane et al., 2009). Black et al. (2004) document a positive shift in mean isotopic values of *G.*  
 402 *ruber* (*foraminifera*) occurred between  $\sim 1000$  and 1100 CE in Cariaco Basin (Fig. 7e). This



positive shift suggests that the Caribbean and tropical North Atlantic were warmer during the MCA. During the early MCA a positive anomaly of Ti also occurs in the Cariaco basin (Haug et al., 2001; Fig. 7d), which is indicative of increased sediment transport by runoff during periods of increased precipitations, characterizing wet conditions. The latter are related to more northerly mean position of ITCZ during this period (Lechleitner et al., 2017). Grey level and wavelet power analysis of the sediment core from Lake Azuei during the MCA period show multidecadal variations, suggesting that multidecadal mode of climate variability, such as AMO, may indeed affect the hydro-climatic conditions in Haiti. Multi-decadal mode variability was observed also in the South American regions during MCA (Viulle et al., 2012, Apaestegui et al., 2014). In addition, the MCA period coincides with positive anomalies of both AMO index and PDO (Mann et al., 2009, Fig. 7g, 7i); which confirms the wet conditions.

The MCA-LIA transition (~1200-1400 CE) corresponds to high climate variability conditions, related to alternations between wet and dry conditions, underlined by the high fluctuations between terrigenous input which correlated with a large variation in the sedimentation rate, Mg Calcite precipitation and organic carbon deposition. The wavelets power analysis of grey level during this period highlights interannual variability, which probably corresponds to Niño3 like, conditions (Fig. 7g). Even if we note a chronological phase shift of 50 years between our record and El Nino 3 index estimated by Mann et al. 2009, which could be due to the errors of extrapolations of our age models during this period, we think that dry conditions during the MCA-LIA transition have been largely influenced by El Niño.

During the LIA, from ~1450 to ~1800 CE, unlike MCA, more negative anomalies of terrigenous input are recorded (Fig. 7b). This reduced transport of terrigenous elements to the lake is related to a decrease in sedimentation rate (Fig. 2b), suggesting a decrease in rainfall patterns. On the other hand, we observed more positive anomalies for Mg-calcite/Ca-calcite ratio during this period (Fig. 7c). Thus, there is formation of Mg-calcite which is a consequence of evaporation related to dry conditions. Other studies have reported evidence of dry conditions in the region during the LIA (Haug et al., 2001; Hodell et al., 2005; Peterson and Haug; 2006, Lane et al., 2009, 2011). The Lagunas Castilla and Salvador records provide further evidence that the LIA may have been, on average, one of the most arid periods in the circum-Caribbean in the last 2000 years (Lane et al., 2009). In the Cariaco basin (Haug et al., 2001), drier conditions are suggested for the LIA by decreased Ti content in core linked to decreased detritus from local rivers (Fig. 7d). The coincident increase in aridity in the geographically distinct locales of the Yucatan Peninsula (Hodell et al., 2005), Panama (Linsley et al., 1994), northern South America (Haug et al., 2001; Peterson and Haug, 2006), Puerto Rico (Nyberg et al., 2001), along the southern slope of the Cordillera Central of the Dominican Republic (Lane et al., 2009; 2011) and Lake Azuei in Haiti (this study) provides evidence that the ITCZ in the Caribbean was located at a more southerly mean annual position during the LIA. The Hydroclimate records discussed by Lechleitner et al. (2017) confirmed also a southward ITCZ shift broadly synchronous with the LIA period. LIA dry conditions are consistent to multidecadal mode highlighted by wavelet



442 analysis of grey level, which corresponds to negative phase of AMO and PDO index (Mann et  
443 al., 2009, Fig. 7f, 7h) and trend to more negative NAO index than MCA period (Trouet et al.,  
444 2009, Fig. 7g).

445 Since we didn't have data for inorganic analysis related to the CWP, we cannot say much about  
446 its climatic variation. However, there was a trend to increase of sedimentation rate (Fig. 2b). In  
447 addition, the lithology profile shows the sediments linked to this period consists of dark  
448 brownish clay with a large amount of OM (Fig. 4). This could be due to the input of sediments  
449 and organic matter into the lake during rainy periods.



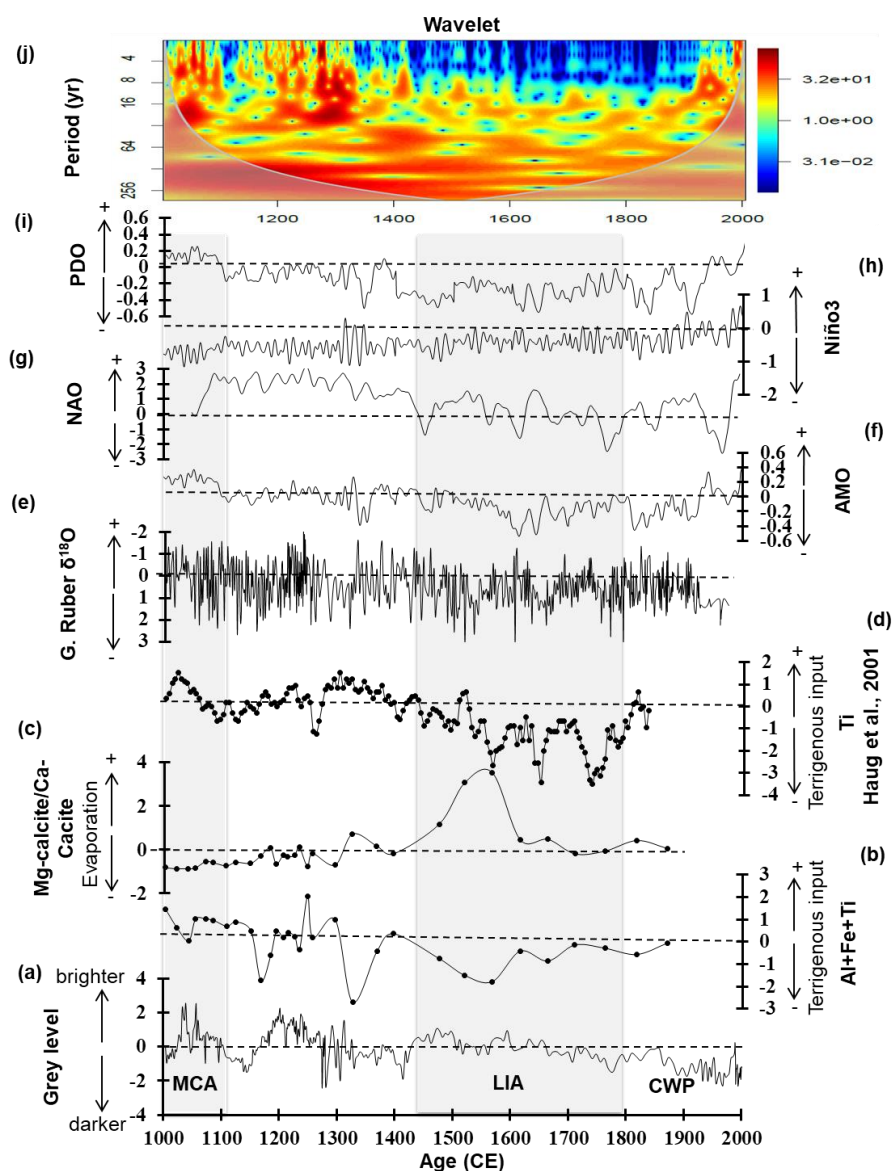


Fig. 7 Comparison of grey scale analysis of the sediment core and sum % Al, Fe, and Ti composition and Mg-calcite/Ca-calcite ratio (this study, (a), (b), (c)) with sediment titanium composite on representing continental runoff through time (Haug et al., 2001, (d)), and *G. ruber*  $\delta^{18}\text{O}$  that reflect sea surface temperature (SST) and Intertropical Convergence Zone (ITCZ) precipitation-related salinity variations over the Caribbean and tropical North Atlantic (Black et al., 2004, (e)), AMO index representing sea surface temperature (SST) anomalies (°C) averaged over the North Atlantic ocean (Mann et al., 2009, (f)), Nino3 temperature anomaly representing SST anomalies in the eastern Pacific ocean (Mann et al., 2009, (g)), NAO index (Trouillet et al.,



2009, (h)), PDO temperature anomaly representing SST anomalies in the eastern Pacific ocean  
 (Mann et al., 2009, (i)) and Wavelet power spectrum: The smooth white line marks the cone of  
 influence; results below that line are unreliable. The color bar indicates the range of wavelet  
 power in the wavelet power spectrum, with hotter colors corresponding to the maximum peaks in  
 wavelet power (j)

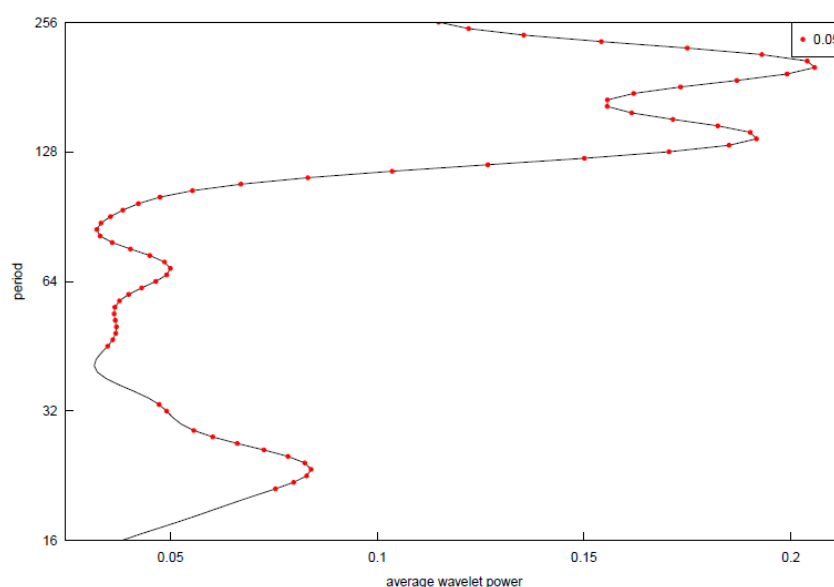


Fig. 8 Spectral analyses of the average wavelet power spectrum of the Fig. 7i

## 5. Conclusions

We use a combination of geochemical and mineralogical data supported by statistical analysis from a core taken in Lake Azuei, to reconstruct hydro-climatic variations in Haiti during the last millennium. The terrigenous elements in the sediments of the lake display a long-term trend toward decreasing content, particularly from 1000 to 1600 CE unlike Mg-calcite neoformation. These opposites' trends suggest progressively drier conditions in Haiti over this period related to a southward shift of the ITCZ. Therefore the MCA period was characterized by more wet conditions in contrast to the LIA period. The MCA-LIA transition was characterized by more unstable conditions, with alternating wet and dry conditions. The CWP is characterized by an increase of sedimentation rate, which is linked to the input of more material into the lake by erosion processes in the lake's catchment as consequence of anthropogenic activities. This study demonstrates also that links exist between precipitations in Haiti and mean changes in the Atlantic and Pacific Oceans through AMO, NAO, PDO and ENSO. In addition temporal correlation of other Caribbean paleoclimate records with our geochemical and mineralogical data, suggests that trends observed in Lake Azuei were controlled by regional climate, likely associated with shifts in the position of the ITCZ. This record provide new detailed information



on hydroclimate variations in Haiti during the last millennium and exhibits trends that are similar to regional patterns identified in other proxy records from the Caribbean and northern tropical Americas. Future studies should focus on other records with higher resolution to better understand interannual and decadal variability.

**Competing interests:** The contact author has declared that neither they nor their co-authors have any competing interests.

## Acknowledgements

We gratefully acknowledge the co-authors for their critical discussions and valuable comments. The acquisition of the cores and their initial analysis was funded through U.S. National Science Foundation grants EAR-1624583 and EAR-1624556. These initial activities involved significant contributions from C.W. Heil, C.K. Hearn, and A.N. Murray. We are especially grateful to our colleagues at the State University of Haiti, D. Boisson, K. Guerrier, and R. Momplaisir for all their help with field logistics and also Eric Calais for supporting this work. The navigation skills and resourcefulness of J. Roy from Pegasus Diving & Services were also key to the success of the coring operations. The participation of Francisco Briceño-Zuluaga in this study is the result of the academic exercise as professor at the Nueva Granada Military University. Francisco Briceño-Zuluaga was also supported by CHARISMA Project (JE0ECCHARI, JEAI-IRD). This research was supported by the “Agence Universitaire de la Francophonie (AUF)” and by the “Projets structurants de formation au Sud” de l’IRD (PSF-CLIMACTS). Geochemical and mineralogical analyses were performed on the ALYSES facility (IRD-SU) that was supported by grants from Région Ile de-France. We would like to thank also LMC14 laboratories for the support in  $^{14}\text{C}$  dating.

## References

- Apaestegui, J., Cruz, F. W., Sifeddine, A., Vuille, M., Espinoza, J. C., Guyot, J. L., ... & Santini, W. (2014). Hydroclimate variability of the northwestern Amazon Basin near the Andean foothills of Peru related to the South American Monsoon System during the last 1600 years. *Climate of the Past*, 10(6), 1967-1981
- Ashby, S. A., Taylor, M. A., & Chen, A. A. (2005). Statistical models for predicting rainfall in the Caribbean. *Theoretical and Applied Climatology*, 82(1), 65-80.
- Benford, B., DeMets, C., & Calais, E. (2012). GPS estimates of microplate motions, northern Caribbean: evidence for a Hispaniola microplate and implications for earthquake hazard. *Geophysical Journal International*, 191(2), 481-490.
- Bird, B. W., Abbott, M. B., Vuille, M., Rodbell, D. T., Stansell, N. D., & Rosenmeier, M. F. (2011). A 2,300-year-long annually resolved record of the South American summer monsoon from the Peruvian Andes. *Proceedings of the National Academy of Sciences*, 108(21), 8583-8588.
- Baumann, K. H., Lackschewitz, K. S., Erlenkeuser, H., Henrich, R., & Jünger, B. (1993). Late



- 519 Quaternary calcium carbonate sedimentation and terrigenous input along the east  
 520 Greenland continental margin. *Marine Geology*, 114(1-2), 13-36.
- 521 Black, D. E., Thunell, R. C., Kaplan, A., Peterson, L. C., & Tappa, E. J. (2004). A 2000-  
 522 year record of Caribbean and tropical North Atlantic hydrographic variability.  
 523 *Paleoceanography*, 19(2).
- 524 Blaauw, M., & Christen, J. A. (2011). Flexible paleoclimate age-depth models using an  
 525 autoregressive gamma process. *Bayesian analysis*, 6(3), 457-474
- 526 Böning, P., Brumsack, H. J., Böttcher, M. E., Schnetger, B., Kriete, C., Kallmeyer, J., &  
 527 Borchers, S. L. (2004). Geochemistry of Peruvian near-surface sediments. *Geochimica et*  
 528 *Cosmochimica Acta*, 68(21), 4429-4451.
- 529 Burn, M. J., & Palmer, S. E. (2014). Solar forcing of Caribbean drought events during the last  
 530 millennium. *Journal of Quaternary Science*, 29(8), 827-836.
- 531 Calvert, S. E., & Pedersen, T. F. (1993). Geochemistry of recent oxic and anoxic marine  
 532 sediments: implications for the geological record. *Marine geology*, 113(1-2), 67-88.
- 533 Cauna, J. D. (2013). Patrimoine et mémoire de l'esclavage en Haïti: les vestiges de la société  
 534 d'habitation coloniale. *In Situ. Revue des patrimoines*, (20).
- 535 Chen, Y. Q., Battisti, D. S., Palmer, T. N., Barsugli, J., & Sarachik, E. S. (1997). A study of  
 536 the predictability of tropical Pacific SST in a coupled atmosphere–ocean model using  
 537 singular vector analysis: The role of the annual cycle and the ENSO cycle. *Monthly*  
 538 *weather review*, 125(5), 831-845.
- 539 Cölfen, H. (2003). Precipitation of carbonates: recent progress in controlled production of  
 540 complex shapes. *Current opinion in colloid & interface science*, 8(1), 23-31.
- 541 Cook, K. H., & Vizy, E. K. (2010). Hydrodynamics of the Caribbean low-level jet and its  
 542 relationship to precipitation. *Journal of Climate*, 23(6), 1477-1494.
- 543 Cormier, M.H., Sloan, H., King, J.W., Boisson, D., Guerrier, K., Hearn, C.K., Heil, C.W., Kelly,  
 544 R.P., Momplaisir, R., Murray, A.N., Sorlien, C.C., Symithe, S.J., Ulysse, S.M.J., &  
 545 Wattrus, N.J. (2018), Late Quaternary Fault-Related Folding, Uplifted Paleoshoreline,  
 546 and Liquefaction Structures: Clues About Transpressional Activity Along the North  
 547 America-Caribbean Plate Boundary From a Comprehensive Seismic Reflection Survey of  
 548 Lake Azuei, Haiti, Fall Meeting of the American Geophysical Union, Washington DC,  
 549 doi: [10.1002/essoar.10500232.1](https://doi.org/10.1002/essoar.10500232.1)
- 550 Curtis, J. H., & Hodell, D. A. (1993). An isotopic and trace element study of ostracods from  
 551 Lake Miragoane, Haiti: A 10,500 year record of paleosalinity and paleotemperature  
 552 changes in the Caribbean. *Washington DC American Geophysical Union Geophysical*  
 553 *Monograph Series*, 78, 135-152.
- 554 Dean, W. E., Rosenbaum, J., & Kaufman, D. (2009). Endogenic carbonate sedimentation in Bear  
 555 Lake, Utah and Idaho, over the last two glacial-interglacial cycles. *Paleoenvironments of*  
 556 *Bear Lake and its catchment: Geological Society of America Special Paper Special*  
 557 *Paper*, 450, 169-196.
- 558 Effler, S. W., & Johnson, D. L. (1987). CALCIUM CARBONATE PRECIPITATION AND



- 559 TURBIDITY MEASUREMENTS IN OTISCO LAKE, NEW YORK 1. *JAWRA Journal*  
 560 *of the American Water Resources Association*, 23(1), 73-79.
- 561 Eisen-Cuadra, Alex Migeul, "Geochemical Record of Global Change in a Closed Basin Lake:  
 562 Étang Saumâtre, Haiti" (2013). *Graduate Doctoral Dissertations*. 130.  
 563 [https://scholarworks.umb.edu/doctoral\\_dissertations/130](https://scholarworks.umb.edu/doctoral_dissertations/130)
- 564 Elfil, H., & Roques, H. (2001). Role of hydrate phases of calcium carbonate on the scaling  
 565 phenomenon. *Desalination*, 137(1-3), 177-186.
- 566 Enfield, D. B., & Mayer, D. A. (1997). Tropical Atlantic sea surface temperature variability  
 567 and its relation to El Niño-Southern Oscillation. *Journal of Geophysical Research:*  
 568 *Oceans*, 102(C1), 929-945.
- 569 Gal, J. Y., Fovet, Y., & Gache, N. (2002). Mechanisms of scale formation and carbon dioxide  
 570 partial pressure influence. Part I. Elaboration of an experimental method and a scaling  
 571 model. *Water Research*, 36(3), 755-763.
- 572 Gamble, D. W., Parnell, D. B., & Curtis, S. (2008). Spatial variability of the Caribbean  
 573 mid-summer drought and relation to north Atlantic high circulation. *International*  
 574 *Journal of Climatology: A Journal of the Royal Meteorological Society*, 28(3), 343-350.
- 575 Giannini, A., Kushnir, Y., & Cane, M. A. (2000). Interannual variability of Caribbean  
 576 rainfall, ENSO, and the Atlantic Ocean. *Journal of Climate*, 13(2), 297-311.
- 577 Goosse H., Klein F. (2021), Les variations climatiques du dernier millénaire,  
 578 Encyclopédie de l'Environnement, [en ligne ISSN 2555-0950] url :  
 579 [https://www.encyclopedie-environnement.org/climat/variations-climatiques-dernier-](https://www.encyclopedie-environnement.org/climat/variations-climatiques-dernier-millenaire/)  
 580 [millenaire/](https://www.encyclopedie-environnement.org/climat/variations-climatiques-dernier-millenaire/).
- 581 Haug, G. H., Hughen, K. A., Sigman, D. M., Peterson, L. C., & Röhl, U. (2001). Southward  
 582 migration of the intertropical convergence zone through the Holocene. *Science*,  
 583 293(5533), 1304-1308.
- 584 Higuera-Gundy, A., Brenner, M., Hodell, D. A., Curtis, J. H., Leyden, B. W., & Binford, M.  
 585 W. (1999). A 10,300 14C yr record of climate and vegetation change from Haiti.  
 586 *Quaternary Research*, 52(2), 159-170.
- 587 Hild, E., & Brumsack, H. J. (1998). Major and minor element geochemistry of Lower  
 588 Aptian sediments from the NW German Basin (core Hoheneggles KB 40). *cretaceous*  
 589 *Research*, 19(5), 615-633.
- 590 Hodell, D. A., Curtis, J. H., Jones, G. A., Higuera-Gundy, A., Brenner, M., Binford, M. W., &  
 591 Dorsey, K. T. (1991). Reconstruction of Caribbean climate change over the past 10,500  
 592 years. *Nature*, 352(6338), 790-793.
- 593 Hodell, D. A., Brenner, M., Curtis, J. H., Medina-Gonzalez, R., Can, E. I. C., Albornaz-Pat,  
 594 A., & Guilderson, T. P. (2005). Climate change on the Yucatan Peninsula during the little  
 595 ice age. *Quaternary Research*, 63(2), 109-121.
- 596 James, K., Cormier, M.H., Sloan, H., Ramsamooj, T., Boisson, D., Guerrier, K., Hearn, C.K.,  
 597 King, J.W., Momplaisir, R., Symithe, S.J., Ulysse, S.M.J., & Wattrus, N.J. (2019).  
 598 Geomorphologic and stratigraphic evidence of ongoing transpressional deformation





- 599 across Lake Azuei (Haiti), *Fall Meeting American Geophysical Union*, San Francisco,  
 600 doi:[10.1002/essoar.10501568.1](https://doi.org/10.1002/essoar.10501568.1).
- 601 Kelts, K., & Hsü, K. J. (1978). Freshwater carbonate sedimentation. In *Lakes* (pp. 295-323).  
 602 Springer, New York, NY.
- 603 Knudsen, M. F., Seidenkrantz, M. S., Jacobsen, B. H., & Kuijpers, A. (2011). Tracking the  
 604 Atlantic Multidecadal Oscillation through the last 8,000 years. *Nature communications*,  
 605 2(1), 1-8.
- 606 Lane, C. S., et al. (2009). "Late-Holocene paleoenvironmental change at mid-elevation on the  
 607 Caribbean slope of the Cordillera Central, Dominican Republic: a multi-site, multi-proxy  
 608 analysis." *Quaternary Science Reviews* 28: 2239-2260.
- 609 Lane, C. S., Horn, S. P., Orvis, K. H., & Thomason, J. M. (2011). Oxygen isotope evidence  
 610 of Little Ice Age aridity on the Caribbean slope of the Cordillera Central, Dominican  
 611 Republic. *Quaternary Research*, 75(3), 461-470.
- 612 Last, W. M. (1982). Holocene carbonate sedimentation in Lake Manitoba, Canada.  
 613 *Sedimentology*, 29(5), 691-704.
- 614 Last, W. M., & De Deckker, P. (1990). Modern and Holocene carbonate sedimentology of two  
 615 saline volcanic maar lakes, southern Australia. *Sedimentology*, 37(6), 967-981.
- 616 Lechleitner, F. A., Breitenbach, S. F., Rehfeld, K., Ridley, H. E., Asmerom, Y., Prufer, K. M., ...  
 617 & Baldini, J. U. (2017). Tropical rainfall over the last two millennia: evidence for a low-  
 618 latitude hydrologic seesaw. *Scientific Reports*, 7(1), 1-9.
- 619 Malmgren, B. A., Winter, A., & Chen, D. (1998). El Nino–southern oscillation and North  
 620 Atlantic oscillation control of climate in Puerto Rico. *Journal of Climate*, 11(10), 2713-  
 621 2717.
- 622 Mann, M. E., Zhang, Z., Rutherford, S., Bradley, R. S., Hughes, M. K., Shindell, D., ... & Ni, F.  
 623 (2009). Global signatures and dynamical origins of the Little Ice Age and Medieval  
 624 Climate Anomaly. *science*, 326(5957), 1256-1260.
- 625 Matthes, H. (1988). Evaluation de la situation de la peche sur les lacs en Haiti. Port-au-  
 626 Prince (Haiti). 84 p. Data ownerFI/FIRA
- 627 Moknatian, M., Piasecki, M., & Gonzalez, J. (2017). Development of geospatial and temporal  
 628 characteristics for Hispaniola's Lake Azuei and Enriquillo using Landsat imagery,  
 629 Remote Sensing, 9, doi: 10.3390/rs9060510.
- 630 Moknatian, M., & Piasecki, M. (2019). Lake volume data analyses: A deep look into the  
 631 shrinking and expansion patterns of Lakes Azuei and Enriquillo, Hispaniola, Hydrology,  
 632 7, 1; doi:10.3390/hydrology7010001.
- 633 Moron, V., Frelat, R., Jean-Jeune, P. K., & Gauchere, C. (2015). Interannual and intra-annual  
 634 variability of rainfall in Haiti (1905–2005). *Climate Dynamics*, 45(3), 915-932.
- 635 Morse, J. W., Arvidson, R. S., & Lüttge, A. (2007). Calcium carbonate formation and  
 636 dissolution. *Chemical reviews*, 107(2), 342-381.
- 637 Müller, G., Irion, G., & Förstner, U. (1972). Formation and Diagenesis of Inorganic Ca-Mg  
 638 Carbonates. *Naturwissenschaften*, 59, 158-164.
- 639 Müller, G., & Wagner, F. (1978). Holocene carbonate evolution in Lake Balaton (Hungary): a



- 640 response to climate and impact of man. *Modern and ancient lake sediments*, 57-81.
- 641 Nan, Z. D., Shi, Z. Y., Qin, M., Hou, W. G., & Tan, Z. C. (2007). Formation process and  
 642 thermodynamic properties of calcite. *Chinese Journal of Chemistry*, 25(5), 592-595.
- 643 Peterson, L. C., & Haug, G. H. (2006). Variability in the mean latitude of the Atlantic  
 644 Intertropical Convergence Zone as recorded by riverine input of sediments to the Cariaco  
 645 Basin (Venezuela). *Palaeogeography, Palaeoclimatology, Palaeoecology*, 234(1), 97-  
 646 113.
- 647 Richey, J. N., Poore, R. Z., Flower, B. P., & Quinn, T. M. (2007). 1400 yr multiproxy record of  
 648 climate variability from the northern Gulf of Mexico. *Geology*, 35(5), 423-426.
- 649 Queralt, I., Julia, R., Plana, F., & Bischoff, J. L. (1997). A hydrous Ca-bearing magnesium  
 650 carbonate from playa lake sediments, Salines Lake, Spain. *American Mineralogist*, 82(7-  
 651 8), 812-819.
- 652 Romero Luna, E. J., & Poteau, D. (2011). *Water level fluctuations of Lake Enriquillo and*  
 653 *Lake Saumatre in response to environmental changes*.
- 654 Schwoerbel, J. (1999). Einführung in die Limnologie.-1-465. *Gustav Fischer) Stuttgart*.
- 655 Solotchina, E. P., & Solotchin, P. A. (2014). Composition and structure of low-temperature  
 656 natural carbonates of the calcite-dolomite series. *Journal of Structural Chemistry*, 55(4),  
 657 779-785.
- 658 Stuiver, M., Reimer, P. J., & Braziunas, T. F. (1998). High-precision radiocarbon age  
 659 calibration for terrestrial and marine samples. *Radiocarbon*, 40(3), 1127-1151.
- 660 Stuiver, M., Reimer, P.J., and Reimer, R.W., 2022, CALIB 8.2 [WWW program] at  
 661 <http://calib.org>, accessed 2022-05-13
- 662 Taylor, S. R., & McLennan, S. M. (1985). The continental crust: its composition and  
 663 evolution.
- 664 Tierney, J. E., Abram, N. J., Anchukaitis, K. J., Evans, M. N., Giry, C., Kilbourne, K. H., ... &  
 665 Zinke, J. (2015). Tropical sea surface temperatures for the past four centuries  
 666 reconstructed from coral archives. *paleoceanography*, 30(3), 226-252.
- 667 Tompa, É., Nyirő-Kósa, I., Rostási, Á., Cserny, T., & Pósfai, M. (2014). Distribution and  
 668 composition of Mg-calcite and dolomite in the water and sediments of Lake Balaton.  
 669 *Central European Geology*, 57(2), 113-136.
- 670 Tribouvillard, N., Algeo, T. J., Lyons, T., & Riboulleau, A. (2006). Trace metals as  
 671 paleoredox and paleoproductivity proxies: an update. *Chemical geology*, 232(1-2), 12-32.
- 672 Valdés, J., Guíñez, M., Castillo, A., & Vega, S. E. (2014). Cu, Pb, and Zn content in sediments  
 673 and benthic organisms from San Jorge Bay (northern Chile): Accumulation and  
 674 biotransference in subtidal coastal systems. *Ciencias Marinas*, 40(1), 45-58.
- 675 Vuille, M., Burns, S. J., Taylor, B. L., Cruz, F. W., Bird, B. W., Abbott, M. B., ... & Novello, V.  
 676 F. (2012). A review of the South American monsoon history as recorded in stable  
 677 isotopic proxies over the past two millennia. *Climate of the Past*, 8(4), 1309-1321.
- 678 Wang, C. (2007). Variability of the Caribbean low-level jet and its relations to climate.  
 679 *Climate dynamics*, 29(4), 411-422.